

Localized Orbitals for Incremental Evaluations of the Correlation Energy within the Domain-Specific Basis Set Approach

Joachim Friedrich*

*Institute for Theoretical Chemistry, University of Cologne, Greinstr. 4,
50939 Cologne, Germany*

Received February 19, 2010

Abstract: A modified version of the Boys localization method is proposed in order to make the domain-specific basis set approach in the framework of the incremental scheme (*J. Chem. Phys.* **2008**, *129*, 244105) generally applicable. The method optimizes the molecular orbitals in one atomic orbital basis set to be similar to localized molecular orbitals in a second atomic orbital basis set under the constraint that the molecular orbitals stay orthonormal. The procedure is tested for RI-MP2 incremental correlation energy expansions for aromatic systems like naphthalene, anthracene, and tetracene as well as for conjugated hydrocarbon chains like C₂₀H₂, C₂₀H₂₂, or *p*-quaterphenyle. For all investigated systems, a rapid convergence of the incrementally expanded correlation energies to the exact RI-MP2 energies is found. Furthermore, the systematic improvability of the approach is demonstrated.

I. Introduction

Density functional theory (DFT) is today's most important quantum chemical method for applications to large systems. The price one has to pay for the increased range of applicability is a lack of systematical improvability. In contrast to DFT methods, wave-function-based correlation methods like many-body perturbation theory (MBPT), configuration interaction (CI), or coupled cluster (CC) are systematically improvable, but their unfavorable scaling with respect to the system size limits their application to small- or medium-sized molecules. The basic idea of local correlation methods is to overcome the unfavorable scaling behavior of the post Hartree–Fock methods by exploiting the local character of the electron correlation. During the past few decades, the development of local correlation methods was an active field in the quantum chemistry community.^{1–22} Within the local domain approximation of Pulay and Saebø,^{3,23} very efficient local versions of MP2,^{24,25} CCSD,⁵ and CCSD(T)²⁶ are available for molecular systems. The extension to periodic systems has been implemented in the CRYSCOR program^{27–29} at the MP2 level of theory. Recently, Subotnik and co-workers proposed the use of

bump-functions to obtain smooth potential energy surfaces for this type of approach.^{6,30,31} The extension of the Pulay approach to MRCI theory was recently proposed by Carter and co-workers.^{14,32}

A conceptually different strategy to obtain a local correlation method is to divide the total system into small fragments and calculate the total energy on the basis of calculations of the small fragments. Within this category, the fragment molecular orbital approach,^{7,33} the divide and conquer approach,^{10,11} the cluster-in-molecule approach,^{22,34} the systematic fragmentation method,¹² and the natural linear scaling coupled cluster^{9,35} were proposed. Another fragment-based local correlation approach is the incremental scheme of Stoll.^{4,36,37} It is a generalization of the Bethe–Goldstone expansion as introduced to the quantum chemistry community by Nesbet.^{1,38,39} In an incremental calculation, the total correlation energy is expanded in a series of correlation energies of small domains:^{40–42}

$$E_{\text{corr}} = \sum_{\substack{\mathbf{X} \\ \mathbf{X} \in \mathcal{P}(\mathbf{D}) \wedge |\mathbf{X}| \leq \mathcal{O}}} \Delta \varepsilon_{\mathbf{X}} \quad (1)$$

where \mathbf{X} is the summation index, \mathbf{D} is the set of domains, $\mathcal{P}(\mathbf{D})$ is the power set of \mathbf{D} , and \mathcal{O} is the order of the expansion. The general increment $\Delta \varepsilon_{\mathbf{X}}$ is defined as

* E-mail: joachim_friedrich@gmx.de.

$$\Delta\varepsilon_X = \varepsilon_X - \sum_{Y \in \mathcal{P}(X) \wedge |Y| < |X|} \Delta\varepsilon_Y \quad (2)$$

where ε_X is the correlation energy of the domain X . Since 1992, the incremental scheme was successfully applied to periodic systems^{43–48} and finite systems.^{40–42,49–52} Recently, the incremental scheme was also successfully applied to describe adsorption processes.^{53–56} The drawback of the method so far was the large amount of hand work required to obtain a correlation energy according to eq 1. Due to the nature of the power set in eq 1, the number of calculations increases very rapidly if the number of domains increases. Since the higher-order increments become negligibly small if the distance of the one-site domains increases, one can safely neglect them without affecting the total accuracy of the calculation. In medium-sized molecules, the number of non-negligible increments is still on the order of 100, and an incremental calculation gets tedious for the one doing computations. To overcome this drawback, we proposed a fully automated implementation of the incremental scheme for molecular systems.⁵¹ With this tool, we were able to investigate the performance of the incremental scheme for MP2, CCSD, CCSD(T), and RCCSD energies with respect to accuracy and efficiency.^{40–42,51,52,57,58} Furthermore, the approach was extended to molecular dipole moments and quadrupole moments,⁵⁹ to treat the core–valence correlation in an efficient manner⁶⁰ and to explicitly correlated MP2 and CCSD theory.⁶¹

Recently, we proposed a domain-specific basis set approach for incremental evaluations of the coupled cluster singles and doubles and perturbative triples (CCSD(T)) energies.^{41,42} It was demonstrated that the approach leads to a significant reduction of RAM and disk space requirements as well as CPU time. Due to the fact that the incremental scheme is inherently parallel, the computations of single increments were distributed over 20–50 nodes of a cheap cluster of standard PCs with a standard 100 megabit Ethernet connection. The key step in this approach is the reduction of the AO basis set in the incremental energy calculations. Since the domains are associated with a local region in space, one can divide the total AO basis set into two parts, the active part, which is spatially close to orbitals in the domain, and the environment, which is the rest of the system. Now we use the large original basis set in the active part and a small basis set in the environment. In order to obtain a set of local and orthogonal orbitals in the new basis set, we perform a Hartree–Fock (HF) calculation with a subsequent Boys localization.⁶² The main problem associated with this procedure is the identification of the occupied orbitals of the domain in the new basis set. In the implementation in ref 42, the mapping of an occupied orbital ϕ_a in the basis \mathcal{B}_1 to the occupied orbital ϕ'_a in the basis \mathcal{B}_2 was accomplished by identifying their centers of charge \bar{R}_a :

$$\bar{R}_a(\mathcal{B}_1) \rightarrow \bar{R}_a(\mathcal{B}_2) \quad (3)$$

This procedure works very well if a unique maximum of the Boys functional exists, e.g., in σ -bonded hydrocarbons, water clusters, etc. For systems with more than one possible

localization maximum, this procedure fails, since the mapping in eq 3 is usually not fulfilled for all occupied orbitals of the system. In this work, a modified Boys localization procedure is implemented, where eq 3 holds for all localized orbitals of a system. The key step of the localization is to use the overlap of the molecular orbitals to a second local set of orbitals, which was previously introduced by Angeli et al.⁶³ as well as by Ahmadi and Røgggen.⁶⁴ Within the framework of the incremental scheme, the approach is tested for various critical systems at the RI-MP2 level using the TURBOMOLE program package.⁶⁵

II. Theory

The incremental scheme and the applied approximations were discussed in detail in refs 43 and 48–50. Therefore, we just give a brief introduction of the applied approximations.

A. The Incremental Method. Equation 1 combines the correlation energies of small subsystems in a systematic manner to obtain a controllable and systematically improvable approximation of the total correlation energy without calculating the correlation energy of the whole system. The starting point of such a calculation is localized HF orbitals obtained by a standard procedure like Boys⁶² or Pipek–Mezey.⁶⁶ Since eq 1 requires disjoint subsets of occupied orbitals, the automatic domain generation of ref 51 is applied to accomplish this task. This method transforms the problem into a graph partitioning problem and applies a standard library routine⁶⁷ to obtain the desired domains.

1. Localized Orbitals and Perturbation Theory. In order to use localized orbitals in combination with an unmodified MP2 code, one has to account for the fact that the Fock matrix is not diagonal in this basis. In the framework of the incremental scheme, this can be done by diagonalization of the Fock matrix in the active space of the domain. In this way, the incremental expansion ensures the canonical condition, since the higher orders correct for the nondiagonal Fock matrix.^{41,42,59}

2. Distance Screening. The distance screening is an essential ingredient for an efficient incremental approach, since the number of calculations $\mathcal{N}_{\text{calc}}$ grows very rapidly with increasing order \mathcal{Q} and number of domains $|\mathcal{D}|$.

$$\mathcal{N}_{\text{calc}} = \sum_{i=1}^{\mathcal{Q}} \binom{|\mathcal{D}|}{i} \quad (4)$$

Therefore, a straightforward application of eq 1 including all possible terms is usually not efficient with respect to CPU time. On the other hand, most of the increments are negligibly small, and one can neglect them without affecting the total accuracy of the calculation. The magnitude of an increment depends on the distances of the one-site domains as well as on the order of the increment (the number of one-site domains in the n -site domain).^{41,42} Therefore, we introduced the order-dependent distance parameter to remove the negligible increments from the expansion:

$$t_{\text{dist}} = \frac{f}{(\mathcal{Q} - 1)^2} \quad \mathcal{Q} \geq 2$$

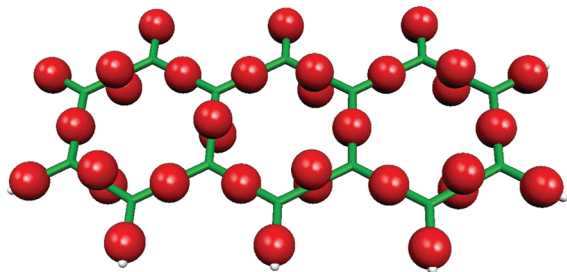


Figure 1. Centers of charge (spheres) for the Boys-localized occupied orbitals of anthracene.

where f is an adjustable parameter with typical values of about 30 Bohr.

3. Domain-Specific Basis Set Approach. The second ingredient for an efficient incremental approach is the domain-specific basis. The basic idea of this approximation is the fact that virtual orbitals far from the domain do not significantly contribute to the correlation energy of an arbitrary domain. Therefore, one can use a smaller basis set for the environment of a domain.^{41,42,68} For a systematic choice of the basis set, we use a sphere with the radius t_{main} for every occupied orbital associated with a given n -site domain (labeled with X). This means we map a set of atoms to every occupied orbital of the domain:

$$\phi_i \rightarrow \{\vec{r}_{i_1}, \vec{r}_{i_2}, \dots\} = A_{\phi_i} \quad (5)$$

where the \vec{r} are coordinates of atoms in the molecule. The active part A_X of an n -site domain is obtained by unifying the sets associated with the orbitals of the domain:

$$A_X = \bigcup_{\phi_i \in X'} A_{\phi_i} \quad X' = \bigcup_{X \in X} X \quad (6)$$

where the sets X' have to be introduced formally to account for the fact that n -site domains are sets of sets of occupied orbitals. Now we use the large original basis for all atoms in A_X , and the rest of the molecule is treated with the smaller basis set. In order to obtain local orthogonal orbitals, a HF calculation with a subsequent localization is performed (vide infra). Besides the reduction of CPU time, the domain-specific basis set approach reduces the number of two-electron integrals significantly and therefore the disk and RAM space requirements.

The key step in this approach is the mapping of a set of local occupied orbitals in one basis to a set of local occupied orbitals in another basis set (eq 3). This mapping step is problematic, since in many real life molecules the set of local orbitals is not unique for symmetry reasons. This can be easily demonstrated using the centers of charge of anthracene (Figure 1): In the ring systems, one can identify the alternating single and double bonds as usually drawn in the Lewis structure. Considering another resonance structure, one can immediately see that there is another equivalent choice for the centers of charge, where the Boys functional has a maximum. The Boys functional just maximizes the distances of the centers of charges, and both localization maxima are equivalent due to symmetry. Therefore, it is usually not predictable to which extremum the Boys localization converges.

B. Template Localization. The standard Boys localization procedure does not necessarily yield occupied orbitals which are sufficiently similar (vide supra), if different AO basis sets are used in a calculation. Therefore, we impose a further condition to accomplish this requirement. The starting point of the procedure is a set of local occupied orbitals (template orbitals) in a small AO basis set \mathcal{B}_2 . The idea is now to make the occupied HF orbitals in a second AO basis \mathcal{B}_1 as equal as possible to the template orbitals without affecting their orthogonality. This can be accomplished by maximizing the functional:

$$D = \sum_k \langle \phi_k^{\mathcal{B}_1} | \phi_k^{\mathcal{B}_2} \rangle \quad (7)$$

where $\phi_k^{\mathcal{B}_1}$ refers to molecular orbitals in the basis \mathcal{B}_1 and $\phi_k^{\mathcal{B}_2}$ represents orbitals in the basis \mathcal{B}_2 . Note that conceptually similar functionals were proposed by Angeli et al.⁶³ and Ahmadi and Røgggen.⁶⁴ A maximization of the functional in eq 7 leads to a set of target functions in the basis \mathcal{B}_1 which are similar to the template functions in the basis \mathcal{B}_2 . In order to preserve the orthogonality, we use orthogonal 2×2 rotations to perform the transformations. This means the matrices O^{ij} which mix the orbitals ϕ_i and ϕ_j have the form

$$O^{ij} = \begin{pmatrix} \cos(\alpha) & \sin(\alpha) \\ -\sin(\alpha) & \cos(\alpha) \end{pmatrix}^{ij} \quad (8)$$

or

$$O^{ij} = \begin{pmatrix} -\cos(\alpha) & \sin(\alpha) \\ \sin(\alpha) & \cos(\alpha) \end{pmatrix}^{ij} \quad (9)$$

where α is the rotation angle. In contrast to the Edmiston–Ruedenberg optimization scheme,⁶⁹ where only 2×2 rotations of the type in eq 8 are applied, we need more flexibility with the second type of rotations in eq 9. A simple example for the need of the second type of rotations is the interchange of two orbitals: We assume that the second set of orbitals is equal to the first set of orbitals, except for a swap of two orbitals. The optimal step is now to swap the two orbitals back, without changing the sign, which corresponds to the second type of rotations. This can be seen explicitly in eq 16 and eq 19 if the corresponding matrix elements are calculated. Equation 19 will find the rotation, whereas eq 16 does not. Since the optimization maximizes the value of D , we have to deal with the second type of rotations in order to include all possible orbital transformations.

With the first matrix, the orbitals read

$$\begin{aligned} \langle \tilde{\phi}_i^{\mathcal{B}_1} | &= \cos(\alpha) \langle \phi_i^{\mathcal{B}_1} | + \sin(\alpha) \langle \phi_j^{\mathcal{B}_1} | \\ \langle \tilde{\phi}_j^{\mathcal{B}_1} | &= -\sin(\alpha) \langle \phi_i^{\mathcal{B}_1} | + \cos(\alpha) \langle \phi_j^{\mathcal{B}_1} | \end{aligned} \quad (10)$$

Inserting the ansatz into eq 7, we obtain

$$\begin{aligned} D_{ij}(\alpha) &= \sum_{k \neq i,j} \langle \phi_k^{\mathcal{B}_1} | \phi_k^{\mathcal{B}_2} \rangle + \cos(\alpha) [\langle \phi_i^{\mathcal{B}_1} | \phi_i^{\mathcal{B}_2} \rangle + \langle \phi_j^{\mathcal{B}_1} | \phi_j^{\mathcal{B}_2} \rangle] \\ &\quad + \sin(\alpha) [\langle \phi_j^{\mathcal{B}_1} | \phi_i^{\mathcal{B}_2} \rangle - \langle \phi_i^{\mathcal{B}_1} | \phi_j^{\mathcal{B}_2} \rangle] \\ &= \sum_{k \neq i,j} \langle \phi_k^{\mathcal{B}_1} | \phi_k^{\mathcal{B}_2} \rangle + \cos(\alpha) A_{ij} + \sin(\alpha) B_{ij} \end{aligned} \quad (11)$$

Now, we define β by

$$\tan \beta = \frac{B_{ij}}{A_{ij}} \quad (12)$$

Using this definition, we arrive after some algebraic manipulations at

$$D_{ij}(\alpha) = \sum_{k \neq i,j} \langle \phi_k^{\beta_1} | \phi_k^{\beta_2} \rangle + \sqrt{A_{ij}^2 + B_{ij}^2} \cos(\alpha - \beta) \quad (13)$$

Since the prefactor of the cosine is always positive, the functional in eq 13 is maximal if the cosine is +1 and minimal if the cosine is -1. This is fulfilled if $\alpha - \beta = 0$ and $\alpha - \beta = \pi$, and thus we get

$$\alpha^{\max} = \beta \quad \alpha^{\min} = \beta + \pi \quad (14)$$

Explicitly, the angle α_{\max} is calculated as

$$\alpha_{ij}^{\max} = \arccos\left(\frac{A_{ij}}{\sqrt{A_{ij}^2 + B_{ij}^2}}\right) \quad (15)$$

Up to now, we found the maximal increase for $D(\alpha)$ for a given pair of functions $\langle \phi_i^{\beta_1} |, \langle \phi_j^{\beta_1} |$. In order to find the maximum increase of $D(\alpha)$ with respect to the choice of all possible orbital pairs i, j , we use the matrix \mathbf{D}^{\max} with the entries

$$\mathbf{D}_{ij}^{\max} = [\mathbf{D}_{ij}^{\max}(\alpha) - D] = -A_{ij} + \sqrt{A_{ij}^2 + B_{ij}^2} \quad (16)$$

The difference between the $\mathbf{D}_{ij}^{\max}(\alpha)$ and D yields the increase of the functional D with respect to a 2×2 rotation of the orbitals i, j . Therefore, the matrix \mathbf{D}^{\max} contains all possible changes. Note that we do not have a dependence on the rotation angle α , since we insert the maximal increase for every orbital pair.

Before we proceed with the final optimization step, we have to consider the second type of rotation in eq 9. In this case, the orbitals read

$$\begin{aligned} \langle \tilde{\phi}_i^{\beta_1} | &= -\cos(\alpha') \langle \phi_i^{\beta_1} | + \sin(\alpha') \langle \phi_j^{\beta_1} | \\ \langle \tilde{\phi}_j^{\beta_1} | &= \sin(\alpha') \langle \phi_i^{\beta_1} | + \cos(\alpha') \langle \phi_j^{\beta_1} | \end{aligned} \quad (17)$$

In the further calculation, we obtain basically the same equations as above. The only difference is the definition of A_{ij} and B_{ij} in the square root:

$$\begin{aligned} A'_{ij} &= -\langle \phi_i^{\beta_1} | \phi_i^{\beta_2} \rangle + \langle \phi_j^{\beta_1} | \phi_j^{\beta_2} \rangle \\ B'_{ij} &= \langle \phi_j^{\beta_1} | \phi_i^{\beta_2} \rangle + \langle \phi_i^{\beta_1} | \phi_j^{\beta_2} \rangle \end{aligned} \quad (18)$$

where the prime is used to indicate rotations of the second type. For the second type of rotations, eq 16 reads

$$\mathbf{D}_{ij}^{\max} = [\mathbf{D}_{ij}^{\max}(\alpha) - D] = -A'_{ij} + \sqrt{A'^2_{ij} + B'^2_{ij}} \quad (19)$$

The final optimization setup is as follows: We search the largest value in \mathbf{D}^{\max} and \mathbf{D}'^{\max} to find the orbital pair with the largest increase of D and perform the associated 2×2 rotation. This is repeated, until all off diagonal elements in \mathbf{D}^{\max} and \mathbf{D}'^{\max} are lower than a given threshold.

The straightforward application of the procedure above might lead to delocalized orbitals, if the optimization

Table 1. List of the Applied Truncation Parameters

dsp	domain size parameter; a rough measure for the size of the domains ⁵¹
t_{con}	connectivity parameter; sets the connectivity for far distant orbitals to zero ⁵¹
t_{main}	the radius around active orbitals to determine the basis for the individual calculations (section II.A.3, ref 41)
core	number of frozen core orbitals
f	parameter for the order dependent distance screening using $\#(\varrho - 1)^2$ (section II.A.2, refs 41, 42)

procedure ends in a local maximum. The reason for this is that the locality of the orbitals comes only implicitly due to the locality of the template orbitals. To overcome this problem, we use Boys orbitals as an initial guess, apply the procedure above, and finally perform a second Boys localization at the end. The first two orthogonal transformations create a set of local orbitals with charge centers close to the template functions. The final Boys localization ensures that the orbitals fulfill an explicit localization criterion; i.e., the Boys functional is maximal.

The composition of these three orthogonal transformations leads to a sufficiently stable algorithm to perform incremental calculations within the domain-specific basis set approach. Note that the orbitals of the composite transformation are not equivalent to Boys orbitals obtained by a standard one-step localization.

III. Computational Details

If nothing else is stated, the geometries were optimized at the RI-BP86/TZVP level of theory using the TURBOMOLE quantum chemistry program package.^{65,70–74} Stationary points were characterized by analyzing the Hessian matrix.⁷⁵ The RI-MP2 energies were computed with the ricc2 module⁷⁶ of TURBOMOLE 5.10. The necessary data such as the Fock matrix, the localization matrix, dipole integrals, as well as the overlap matrix of two different AO basis sets were obtained by an interface to a development version of TURBOMOLE.

A. Incremental Calculations. The threshold for the maximum values in the matrices \mathbf{D}^{\max} and \mathbf{D}'^{\max} was set to 10^{-8} in the template localization step, whereas the Boys localizations were converged to 10^{-11} . The occupied orbitals in the two basis sets were identified by their centers of charge with an identification tolerance of 0.1 Bohr. In the incremental energy evaluations, the RI basis (cbas) of the large original basis set was used for the total system. To get an overview of the applied truncation parameters in our incremental calculations, we included a list of the parameters with a short description (Table 1). In the environment, the SVP basis was applied for all systems in this study.

IV. Applications

A critical test for the stability of the proposed procedure is the evaluation of increments within the domain-specific basis set approach. First, the incremental scheme requires a large number of calculations; e.g., in order to get a single correlation energy, it is not unusual that a few hundred correlation calculations are necessary. In the domain-specific

Table 2. Convergence of the Incremental RI-MP2 Correlation Energies^a

order	C ₁₀ H ₂₂			C ₂₀ H ₄₂			C ₂₀ H ₂₂		
	$E_{\text{corr}}(l)$ [a.u.]	error [kcal/mol]	E_{corr} [%]	$E_{\text{corr}}(l)$ [a.u.]	error [kcal/mol]	E_{corr} [%]	$E_{\text{corr}}(l)$ [a.u.]	error [kcal/mol]	E_{corr} [%]
TZVP									
1	-1.188660	209.80	78.05	-2.293514	461.38	75.72	-1.995851	489.70	71.89
2	-1.520772	1.39	99.85	-3.021870	4.33	99.77	-2.761895	9.00	99.48
3	-1.523373	-0.24	100.03	-3.030365	-1.00	100.05	-2.775034	0.75	99.96
exact	-1.522990			-3.028767			-2.776232		
QZVP									
1	-1.464292	254.13	78.34	-2.826150	558.80	76.04	-2.460658	587.39	72.44
2	-1.867051	1.39	99.88	-3.710525	3.84	99.84	-3.381958	9.26	99.57
3	-1.869324	-0.04	100.00	-3.716863	-0.14	100.01	-3.395008	1.08	99.95
exact	-1.869267			-3.716647			-3.396722		

^a core = 10 (C₁₀H₂₂), core = 20 (C₂₀H₄₂, C₂₀ H₂₂); dsp = 4; t_{main} = 3 Bohr; f = 25 Bohr (C₁₀H₂₂, C₂₀H₄₂), f = 30 Bohr (C₂₀ H₂₂); t_{con} = 3 Bohr.

basis set, this means that the localization has to work for every single calculation. Second, the structure of the basis for the calculation in the n -site domains is more complicated, since there might be several regions with different basis sets in the molecule; e.g., in higher order domains, the orbital domains are not necessarily local anymore. In cases where the Boys functional has several symmetry equivalent maxima like in benzene, it is not predictable and not controllable to which maximum the Boys localization will converge. With the proposed algorithm, we were able to overcome this drawback for all cases tested so far.

The main goal of this work is the test of the potential accuracy of the domain-specific basis set approach in combination with the template localization. Within the efficient RI-MP2 routines in TURBOMOLE,^{76,77} there is no need to make local approximations in the correlation part for the molecules in this study, since the HF calculation consumes a large part of the CPU time in our calculations. Clearly, this will change if coupled cluster methods are used. However, to test the performance of the approach with respect to the accuracy on a large set of molecules, we decided to use MP2, since when the domain-specific basis set approach is used the convergence of the MP2 energies is similar to the convergence of the coupled cluster energies.^{41,42,68}

A. Boys Systems. The first issue to study is the performance of the new approach for systems where no problems with the ambiguity of the localization exist, i.e., Boys systems, in order to investigate how the proposed procedure might affect the accuracy in these cases.

1. Hydrocarbons. An easy test case for local correlation methods is the use of unbranched hydrocarbon chains. In Table 2, we present the results for decane, eicosane, and the unsaturated C₂₀H₂₂ in the TZVP and in the QZVP basis sets, respectively. For both saturated hydrocarbons in the TZVP basis set, the convergence of the incremental series is fast, and a third-order expansion is sufficient to obtain chemical accuracy of about 1 kcal/mol. The relative correlation energy is 100.03% and 100.05% for decane and eicosane, respectively. Increasing the basis set to the quadruple- ζ level slightly improves the accuracy of the incrementally expanded energy. At third-order level, the errors are -0.04 and -0.14 kcal/mol.

Table 3. Convergence of the Incremental RI-MP2 Correlation Energies of the (H₂O)₁₃ Cluster in Figure 2 Using the aug-cc-pVXZ Basis Set Series of Dunning and Co-Workers^{79,80 a}

order	$E_{\text{corr}}(l)$ [a.u.]	error [kcal/mol]	E_{corr} [%]
aug-cc-pVDZ			
1	-2.824690	72.96	96.05
2	-2.942911	-1.22	100.07
3	-2.940631	0.21	99.99
exact	-2.940959		
aug-cc-pVTZ			
1	-3.456064	79.23	96.48
2	-3.583812	-0.94	100.04
3	-3.582025	0.19	99.99
exact	-3.582320		
aug-cc-pVQZ			
1	-3.682562	78.49	96.72
2	-3.808779	-0.71	100.03
3	-3.807413	0.14	99.99
exact	-3.807641		

^a core = 13, dsp = 4 Bohr, t_{main} = 3 Bohr, f = 25 Bohr, t_{con} = 3 Bohr.

More difficult examples for local correlation methods are conjugated π systems. Therefore, we study C₂₀H₂₂ with alternating single and double bonds. Using the same truncation parameters as for the saturated hydrocarbons, the errors for the unsaturated C₂₀ chain are 0.75 kcal/mol in the TZVP basis set and 1.08 kcal/mol in the QZVP basis set. Comparing the accuracy of the RI-MP2 correlation energies for the saturated hydrocarbons and the unsaturated hydrocarbon, we find a slightly higher accuracy for saturated hydrocarbons. We note that the accuracy can be increased by increasing the domain size parameter (dsp) or the radius for the basis set truncation (t_{main}).

2. Water Cluster. The incremental scheme yields very accurate results for molecular clusters. With the domain-specific basis set approach, it was demonstrated earlier that the incremental scheme can be applied very efficiently for water clusters in the framework of coupled cluster.^{42,68} Table 3 shows the convergence of the incremental RI-MP2 correlation energies with respect to the exact RI-MP2 correlation energy for the aug-cc-pVXZ (X = D,T,Q) basis set series of Dunning et al.^{79,80} The accuracy of the incremental expansions is similar for the applied aug-cc-pVXZ basis sets. At second order, the errors are on the order of 1 kcal/mol,

Table 4. Dependence of RI-MP2 Correlation Energies, Errors, and Relative Correlation Energies of $C_{20}H_2$ on the Truncation Parameters of Table 1^a

entry no.	order	dsp	f [Bohr]	t_{main} [Bohr]	$E_{\text{corr}}(l)$ [a.u.]	error [kcal/mol]	E_{corr} [%]
basis = TZVP							
1	3	4	25	3	-2.640592	3.15	99.81
2	3	4	30	3	-2.643350	1.42	99.91
3	4	4	30	3	-2.644079	0.96	99.94
4	3	4	40	3	-2.643461	1.35	99.92
5	4	4	40	3	-2.644190	0.89	99.95
6	3	5	25	3	-2.643765	1.15	99.93
7	3	6	25	3	-2.644735	0.55	99.97
8	3	4	25	5	-2.640372	3.28	99.80
9	4	4	25	5	-2.643584	1.27	99.92
10	3	4	30	5	-2.643920	1.06	99.94
11	4	4	30	5	-2.644121	0.93	99.94
12	3	4	40	5	-2.643965	1.03	99.94
13	4	4	40	5	-2.644167	0.90	99.95
14	3	5	40	5	-2.644633	0.61	99.96
15	4	5	40	5	-2.645062	0.34	99.98
exact					2.645605		
basis = QZVP							
16	3	5	40	5	-3.201505	0.73	99.96
exact					-3.202670		

^a core = 20, $t_{\text{con}} = 3$ Bohr.

and at third order, they are below 1 kcal/mol (0.21, 0.19, 0.14 kcal/mol).

Finally, we conclude that the convergence of the incremental series in the domain-specific basis-set approach using template localized orbitals is sufficiently fast, and chemically accurate results can be obtained for the Boys systems.

B. Non-Boys-Systems. The focus of this work is to demonstrate the performance of the template localization for the cases where the simple procedure outlined in ref 42 does not work, i.e., non-Boys systems. Therefore, we applied the approach to various systems of chemical interest such as conjugated π systems and aromatic compounds with a highly delocalized nature.

1. $C_{20}H_2$. As a first critical test system, we applied the domain-specific basis set approach in combination with the template localization to $C_{20}H_2$. This molecule is a challenge for local correlation methods since it has alternating single and triple bonds. Furthermore, the treatment of triple bonds is not possible within the domain-specific basis set approach, if standard Boys orbitals are used. The problems occur in the identification of the localized orbitals within two different basis sets, since the localization is not unique for triple bonds. For example, maximizing the distances of the charge centers in a triple bond results in a triangle, which can be rotated around the bond axis without changing the Boys functional. Practically, this means that the program terminates with an error since

$$|\vec{R}_a(\mathcal{B}_1) - \vec{R}_a(\mathcal{B}_2)| < 0.1 \text{ Bohr}$$

is usually not fulfilled for Boys orbitals. With the proposed localization scheme, the identification of the occupied orbitals within two different basis sets could be done for all molecules and for all increments in this study. The performance of the incremental scheme in combination with template-localized orbitals is presented in Table 4 for various truncation

parameters (order, dsp, f , and t_{main}). Using dsp = 4, $f = 25$, and $t_{\text{main}} = 3$ as for the saturated hydrocarbon compounds above, the error of the RI-MP2/TZVP correlation energy is 3.15 kcal/mol at third order. Increasing the order-dependent distance threshold f from 25 to 30 Bohr, the error decreases by about a factor of 2 to 1.42 kcal/mol. A further increase of f to 40 Bohr does not significantly improve the energy (entry 4). The error at fourth order is 0.96 kcal/mol for $f = 30$ and 0.89 kcal/mol for $f = 40$ (entries 3 and 5). This small change in the energies with respect to the distance threshold f indicates that the significant increments are included already for $f = 30$. This observation is equivalently true when comparing the entry pairs 10 and 12 and 11 and 13 with a larger t_{main} . Increasing the domain size from dsp = 4 to dsp = 6 decreases the error to 0.55 kcal/mol (entry 7). Increasing the radius for the basis set truncation from $t_{\text{main}} = 3$ to $t_{\text{main}} = 5$ decreases the error to 1.06 kcal/mol for the third order calculation (entry 10). At the fourth order level, the error is 0.93 kcal/mol (entry 11). For dsp = 5 and $t_{\text{main}} = 5$, the error is 0.61 kcal/mol at third order and 0.34 kcal/mol at fourth order (entries 14 and 15). Comparing entries 1 and 8, we find a slightly smaller fraction of the correlation energy for the calculation with the larger t_{main} in entry 8. This behavior can be explained by the tight distance truncation with $f = 25$ which causes an error around 2 kcal/mol. If we compare the corresponding entry pairs with $f = 30$ (entries 2 and 10), we find that the increase of t_{main} from 3 to 5 yields again a higher accuracy. These findings can be explained by the fact that a larger t_{main} can lead to larger contributions of the individual increments. If the distance truncation is as serious as in entries 1 and 8, it is not surprising that a larger t_{main} does not improve the total accuracy, since the sum of the neglected increments is large for $f = 25$ and it was slightly increased by the increase of t_{main} . Increasing the basis set from TZVP to QZVP increases the error slightly from 0.61 to 0.73 kcal/mol (entry 16). Note that the change in the total energy is ca. 350 kcal/mol in going from TZVP to QZVP.

From these findings, it is evident that the truncation parameters can be used to control the accuracy of the incremental scheme in a systematic manner and that the template localization works sufficiently well for this difficult system.

2. Polycyclic Aromatic Hydrocarbons. Next, the proposed localization procedure is tested for polycyclic aromatic hydrocarbons (Figure 2). Therefore, we check the performance of the approach for naphthalene, anthracene, and tetracene (Table 5). Considering the accuracy of the incremental series, we obtain errors of about 1 kcal/mol for a third-order calculation using the same thresholds as for the saturated hydrocarbons above. The relative correlation energy ranges from 99.97% to 100.05% in the TZVP basis set. If the larger QZVP basis set is used, the errors increase slightly to -0.88 and -1.09 kcal/mol for naphthalene and anthracene, respectively. Due to the accuracy of the results, we conclude that polycyclic aromatic hydrocarbons can be treated with the incremental scheme. As expected for such highly delocalized systems, they are slightly more difficult to treat than their saturated counterparts.

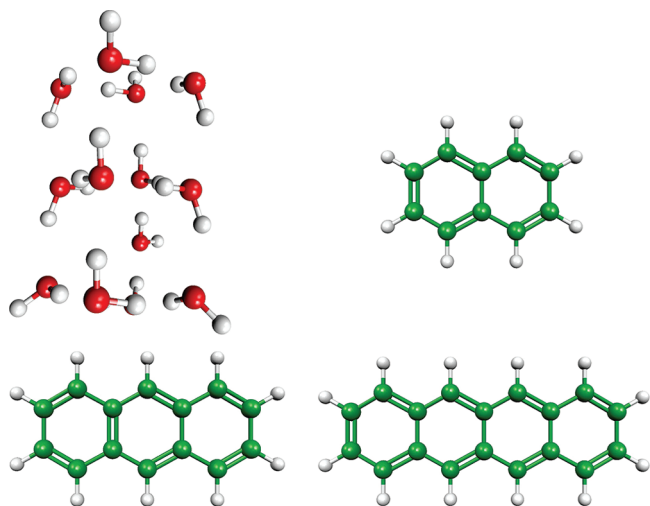


Figure 2. RI-BP86/TZVP optimized structures of naphthalene, anthracene, and tetracene. The geometry of the $(\text{H}_2\text{O})_{13}$ cluster was taken from ref 78.

A further interesting test system for the localization method is the *p*-quaterphenyle molecule in Figure 3. The results of the third order calculations for different truncation parameters are given in Table 6. In this case, the results clearly indicate that one should not use the same truncation parameters as for the saturated hydrocarbons. On the other hand, the quality of the third order energies can be improved by increasing the domain sizes and the radius for the basis set truncation. With sufficiently large values for dsp and t_{main} , one can obtain 99.94% of the correlation energy. The error is 1.33 kcal/mol, which is slightly above the desired error of 1 kcal/mol. However, this is a critical molecule for local correlation approaches, and the accuracy is still reasonable.

3. *Oligopeptide.* As a final example, we included the oligopeptide in Figure 4. For peptides without aromatic groups, the domain-specific basis set approach can be applied in combination with Boys orbitals as demonstrated in ref 41. To obtain a critical test of the proposed localization procedure, we included histidine, tryptophan, and phenylalanine. The convergence of the incremental series for the RI-MP2/TZVP correlation energy for this system is given in Table 7 using two sets of truncation parameters. The convergence of the incremental series is fast for both parameter sets since 99.89% and 99.95% of the correlation

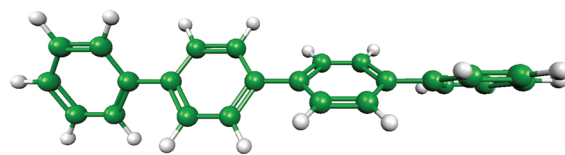


Figure 3. RI-BP86/TZVP optimized structure of *p*-quaterphenyle.

Table 6. Dependence of RI-MP2/TZVP Correlation Energies, Errors and Relative Correlation Energies of *p*-Quaterphenyle on the Parameters of Table 1^a

order	dsp	f [Bohr]	t_{main} [Bohr]	$E_{\text{corr}}(i)$ [a.u.]	error [kcal/mol]	E_{corr} [%]
3	4	∞	3	−3.303295	−17.19	100.84
3	5	∞	6	−3.256601	12.11	99.41
3	6	35	6	−3.273790	1.33	99.94
exact				−3.275906		

^a core = 24, $t_{\text{con}} = 3$ Bohr.

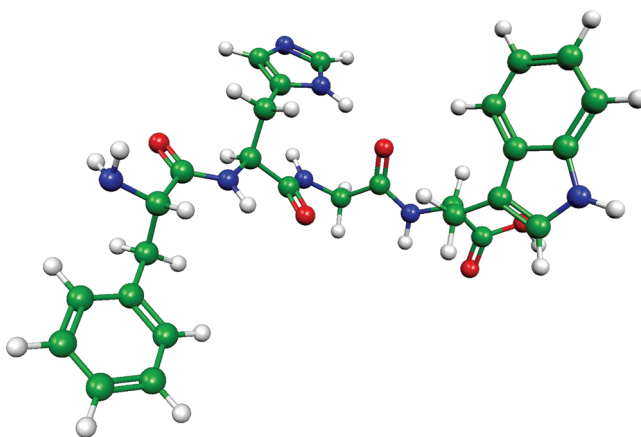


Figure 4. RI-BP86/SV(P) optimized structure of an oligopeptide.

energy are recovered at third order. At fourth order, 99.95% and 99.99% of the correlation energy are recovered. The absolute errors are still above 1 kcal/mol except for the fourth order calculation in combination with $\text{dsp} = 6$ and $t_{\text{main}} = 5$ Bohr. The reason for the larger absolute error is the magnitude of the correlation energy.

Since the convergence of the MP2 correlation energies in the domain-specific basis set approach is similar to the convergence of the corresponding coupled cluster energies

Table 5. Convergence of the Incremental RI-MP2 Correlation Energies for Naphthalene, Anthracene, and Tetracene^a

order	naphthalene			anthracene			tetracene		
	$E_{\text{corr}}(i)$ [a.u.]	error [kcal/mol]	E_{corr} [%]	$E_{\text{corr}}(i)$ [a.u.]	error [kcal/mol]	E_{corr} [%]	$E_{\text{corr}}(i)$ [a.u.]	error [kcal/mol]	E_{corr} [%]
TZVP									
1	−0.904435	284.87	66.58	−1.217251	426.96	64.14	−1.401001	651.19	57.45
2	−1.350451	5.00	99.41	−1.879245	11.55	99.03	−2.407246	19.76	98.71
3	−1.359066	−0.41	100.05	−1.898451	−0.50	100.04	−2.437892	0.53	99.97
exact	−1.358411			−1.897658			−2.438732		
QZVP									
1	−1.118346	342.97	67.17	−1.506995	512.63	64.85			
2	−1.655905	5.65	99.46	−2.303540	12.79	99.12			
3	−1.666305	−0.88	100.08	−2.325659	−1.09	100.07			
exact	−1.664910			−2.323917					

^a Naphthalene: core = 10, $\text{dsp} = 4$, $t_{\text{main}} = 3$ Bohr, $f = \text{inf}$ Bohr, $t_{\text{con}} = 3$ Bohr. Anthracene: core = 14, $\text{dsp} = 4$, $t_{\text{main}} = 3$ Bohr, $f = 30$ Bohr, $t_{\text{con}} = 3$ Bohr. Tetracene: core = 18, $\text{dsp} = 4$, $t_{\text{main}} = 3$ Bohr, $f = 30$ Bohr, $t_{\text{con}} = 3$ Bohr.

Table 7. Convergence of the Incremental RI-MP2/TZVP Correlation Energies for the Oligopeptide in Figure 4^a

order	$E_{\text{corr}}(l)$ [a.u.]	error [kcal/mol]	E_{corr} [%]
dsp = 4, $t_{\text{main}} = 3$ Bohr			
1	-4.609373	944.28	75.39
2	-6.103895	6.45	99.83
3	-6.107536	4.17	99.89
4	-6.111360	1.77	99.95
dsp = 6, $t_{\text{main}} = 5$ Bohr			
1	-4.758638	850.61	77.83
2	-6.109521	2.92	99.92
3	-6.111255	1.83	99.95
4	-6.113515	0.41	99.99
exact	-6.114175		

^a core = 40, dsp=4, $t_{\text{main}} = 3$ Bohr, $f = 30$ Bohr, $t_{\text{con}} = 3$ Bohr.

it seems to be a promising goal to use template localized orbitals at the coupled cluster level. We note that a significant reduction of the total CPU time was achieved with the domain-specific basis set approach at the CCSD(T) level.⁴¹

V. Conclusion

We implemented a modified version of the Boys localization which can be applied to extend the domain-specific basis set approach to aromatic systems, where the original approach does not work. It was shown for aromatic systems like naphthalene, anthracene, and tetracene and conjugated hydrocarbon chains like C₂₀H₂, C₂₀H₂₂, and *p*-quaterphenyle that the localization procedure works sufficiently well. The accuracy of the incremental RI-MP2 correlation energies is close to a chemical accuracy of 1 kcal/mol for these difficult systems, if appropriate truncation parameters are used. Furthermore, it has been demonstrated that increasing the domain sizes or increasing t_{main} systematically improves the accuracy of the calculation. In the future, we plan to combine the template localization with the CCSD(T) implementation of the incremental scheme, to obtain a generally applicable systematically improvable and efficient incremental CCSD(T) method.

Acknowledgment. This work was supported by the German Research Foundation (DFG) through priority program 1145 and SFB 624. The author would like to acknowledge Prof. M. Dolg and Dr. A. Engels-Putzka for various discussions and carefully reading the manuscript, Prof. T. Helgaker for discussing the localization procedure, Dr. D. P. Tew for the required data interfaces to TURBO-MOLE, and T. Kjærgaard for an interface to the required overlap integrals in DALTON.

References

- Nesbet, R. K. *Phys. Rev.* **1967**, *155*, 51.
- Förner, W.; Ladik, J.; Otto, P.; Cizek, J. *Chem. Phys.* **1985**, *97*, 251.
- Pulay, P.; Saebø, S. *Theor. Chim. Acta.* **1986**, *69*, 357.
- Stoll, H. *Chem. Phys. Lett.* **1992**, *191*, 548.
- Hampel, C.; Werner, H.-J. *J. Chem. Phys.* **1996**, *104*, 6286.
- Subotnik, J. E.; Head-Gordon, M. *J. Chem. Phys.* **2005**, *123*, 64108.
- Fedorov, D. G.; Kitaura, K. *J. Chem. Phys.* **2004**, *121*, 2483.
- Gordon, M. S.; Mullin, J. M.; Pruitt, S. R.; Roskop, L. B.; Slipchenko, L. V.; Boatz, J. A. *J. Phys. Chem. B* **2009**, *113*, 9646.
- Flocke, N.; Bartlett, R. J. *J. Chem. Phys.* **2004**, *121*, 10935.
- Kobayashi, M.; Imamura, Y.; Nakai, H. *J. Chem. Phys.* **2007**, *127*, 074103.
- Kobayashi, M.; Nakai, H. *J. Chem. Phys.* **2008**, *129*, 044103.
- Deev, V.; Collins, M. A. *J. Chem. Phys.* **2005**, *122*, 154102.
- Li, S.; Shen, J.; Li, W.; Jiang, Y. *J. Chem. Phys.* **2006**, *125*, 074109.
- Walter, D.; Szilva, A. B.; Niedfeld, K.; Carter, E. A. *J. Chem. Phys.* **2002**, *117*, 1982.
- Auer, A. A.; Nooijen, M. *J. Chem. Phys.* **2006**, *125*, 024104.
- Weijo, V.; Manninen, P.; Jørgenson, P.; Christiansen, O.; Olsen, J. *J. Chem. Phys.* **2007**, *127*, 074106.
- Doser, B.; Lambrecht, D. S.; Ochsenfeld, C. *Phys. Chem. Chem. Phys.* **2008**, *10*, 3335.
- Kamiya, M.; Hirata, S.; Valiev, M. *J. Chem. Phys.* **2008**, *128*, 074103.
- Dahlke, E. E.; Leverentz, H. R.; Truhlar, D. G. *J. Chem. Theory Comput.* **2008**, *4*, 33.
- Russ, N. J.; Crawford, T. D. *Phys. Chem. Chem. Phys.* **2008**, *10*, 3345.
- Li, W.; Li, S. *J. Chem. Phys.* **2004**, *121*, 6649.
- Li, W.; Piecuch, P.; Gour, J. R.; Li, S. *J. Chem. Phys.* **2009**, *131*, 114109.
- Saebø, S.; Pulay, P. *Annu. Rev. Phys. Chem.* **1993**, *44*, 213.
- Schütz, M.; Hetzer, G.; Werner, H. J. *J. Chem. Phys.* **1999**, *111* (13), 5691.
- Adler, T. B.; Werner, H.-J.; Manby, F. R. *J. Chem. Phys.* **2009**, *130*, 054106.
- Schütz, M. *J. Chem. Phys.* **2000**, *113* (22), 9986.
- Pisani, C.; Busso, M.; Capecchi, G.; Casassa, S.; Dovesi, R.; Maschio, L.; Zicovich-Wilson, C.; Schütz, M. *J. Chem. Phys.* **2005**, *122* (9).
- Maschio, L.; Usvyat, D.; Manby, F. R.; Casassa, S.; Pisani, C.; Schütz, M. *Phys. Rev. B* **2007**, *76* (7).
- Usvyat, D.; Maschio, L.; Manby, F. R.; Casassa, S.; Schütz, M.; Pisani, C. *Phys. Rev. B* **2007**, *76* (7).
- Subotnik, J. E.; Sodt, A.; Head-Gordon, M. *J. Chem. Phys.* **2006**, *125*, 074116.
- Subotnik, J. E.; Sodt, A.; Head-Gordon, M. *J. Chem. Phys.* **2008**, *128*, 034103.
- Chwee, T. S.; Szilva, A. B.; Lindh, R.; Carter, E. A. *J. Chem. Phys.* **2008**, *128*, 224106.
- Fedorov, D. G.; Kitaura, K. *J. Chem. Phys.* **2005**, *123*, 134103.
- Li, W.; Piecuch, P.; Gour, J. R. *Theory and Applications of Computational Chemistry - 2008, AIP Conference Proceedings*, 2009; Vol. 1102, p 68.
- Hughes, T. F.; Flocke, N.; Bartlett, R. J. *J. Phys. Chem. A* **2008**, *112*, 5994.
- Stoll, H. *Phys. Rev. B: Condens. Matter Mater. Phys.* **1992**, *46*, 6700.

- (37) Stoll, H. *J. Chem. Phys.* **1992**, 97, 8449.
- (38) Nesbet, R. K. *Phys. Rev.* **1968**, 175, 2.
- (39) Nesbet, R. K. *Adv. Chem. Phys.* **1969**, 14, 1.
- (40) Friedrich, J.; Hanrath, M.; Dolg, M. *J. Phys. Chem. A* **2007**, 111, 9830.
- (41) Friedrich, J.; Dolg, M. *J. Chem. Phys.* **2008**, 129, 244105.
- (42) Friedrich, J.; Dolg, M. *J. Chem. Theory Comput.* **2009**, 5, 287.
- (43) Yu, M.; Kalvoda, S.; Dolg, M. *Chem. Phys. Lett.* **1997**, 224, 121.
- (44) Abdurahman, A.; Shukla, A.; Dolg, M. *J. Chem. Phys.* **2000**, 112, 4801.
- (45) Stoll, H.; Paulus, B.; Fulde, P. *J. Chem. Phys.* **2005**, 123, 144108.
- (46) Albrecht, M.; Paulus, B.; Stoll, H. *Phys. Rev. B* **1997**, 56, 7339.
- (47) Doll, K.; Dolg, M.; Fulde, P.; Stoll, H. *Phys. Rev. B* **1995**, 52, 4842.
- (48) Doll, K.; Dolg, M.; Fulde, P.; Stoll, H. *Phys. Rev. B* **1997**, 55, 10282.
- (49) Kalvoda, S.; Paulus, B.; Dolg, M.; Stoll, H.; Werner, H.-J. *Phys. Chem. Chem. Phys.* **2001**, 3, 514.
- (50) Paulus, B. *Int. J. Quantum Chem.* **2004**, 100, 1026.
- (51) Friedrich, J.; Hanrath, M.; Dolg, M. *J. Chem. Phys.* **2007**, 126, 154110.
- (52) Friedrich, J.; Hanrath, M.; Dolg, M. *Chem. Phys.* **2007**, 338, 33.
- (53) Müller, C.; Herschend, B.; Hermansson, K.; Paulus, B. *J. Chem. Phys.* **2008**, 128, 214701.
- (54) Müller, C.; Paulus, B.; Hermansson, K. *Surf. Sci.* **2009**, 603, 2619.
- (55) Müller, C.; Hermansson, K.; Paulus, B. *Chem. Phys.* **2009**, 362, 91.
- (56) Schmitt, I.; Fink, K.; Staemmler, V. *Phys. Chem. Chem. Phys.* **2009**, 11, 11196.
- (57) Friedrich, J.; Hanrath, M.; Dolg, M. *Chem. Phys.* **2008**, 346, 266.
- (58) Friedrich, J.; Hanrath, M.; Dolg, M. *J. Phys. Chem. A* **2008**, 112, 8762.
- (59) Friedrich, J.; Coriani, S.; Helgaker, T.; Dolg, M. *J. Chem. Phys.* **2009**, 131, 154102.
- (60) Friedrich, J.; Walczak, K.; Dolg, M. *Chem. Phys.* **2009**, 356, 47.
- (61) Friedrich, J.; Tew, D.; Klopper, W.; Dolg, M. *J. Chem. Phys.* **2010**, 132, 164114.
- (62) Foster, J. M.; Boys, S. F. *Rev. Mod. Phys.* **1960**, 32, 300.
- (63) Angeli, C.; Del Re, G.; Persico, M. *Chem. Phys. Lett.* **1995**, 233, 102.
- (64) Ahmadi, G. R.; Røgggen, I. *Theor. Chem. Acc.* **1997**, 97, 41.
- (65) Alrichs, R.; Bär, M.; Baron, H.-P.; Bauernschmitt, R.; Böcker, S.; Ehrig, M.; Eichkorn, K.; Elliott, S.; Furche, F.; Haase, F.; Häser, M.; Horn, H.; Huber, C.; Huniar, U.; Kölmel, C.; Kollwitz, M.; Ochsenfeld, C.; Öhm, H.; Schäfer, A.; Schneider, U.; Treutler, O.; von Arnim, M.; Weigend, F.; Weis, P.; Weiss, H. *Turbomole 5.10*; Institut für Physikalische Chemie, Universität Karlsruhe: Karlsruhe, Germany, 2008.
- (66) Pipek, J.; Mezey, P. G. *J. Chem. Phys.* **1989**, 90, 4916.
- (67) Karypis, G.; Kumar, V. *SIAM J. Sci. Comput.* **1998**, 20 (1), 359.
- (68) Friedrich, J.; Hanrath, M.; Dolg, M. *Z. Phys. Chem.* **2010**, in press.
- (69) Edmiston, C.; Ruedenberg, K. *Rev. Mod. Phys.* **1963**, 35, 457.
- (70) Becke, A. D. *Phys. Rev. A* **1988**, 38 (6), 3098.
- (71) Perdew, J. P. *Phys. Rev. B* **1986**, 33 (12), 8822.
- (72) Treutler, O.; Ahlrichs, R. *J. Chem. Phys.* **1995**, 102, 346.
- (73) Eichkorn, K.; Treutler, O.; Oehm, H.; Haeser, M.; Ahlrichs, R. *Chem. Phys. Lett.* **1995**, 240, 283.
- (74) Eichkorn, K.; Weigend, F.; Treutler, O.; Ahlrichs, R. *Theor. Chem. Acc.* **1997**, 97, 119.
- (75) Deglmann, P.; May, K.; Furche, F.; Ahlrichs, R. *Chem. Phys. Lett.* **2004**, 384, 103.
- (76) Weigend, F.; Hättig, C. *J. Chem. Phys.* **2000**, 113, 5154.
- (77) Weigend, F.; Häser, M.; Patzelt, H.; Ahlrichs, R. *Chem. Phys. Lett.* **1998**, 294, 143.
- (78) Bulusu, S.; Yoo, S.; Apra, E.; Xantheas, S.; Zeng, X. C. *J. Phys. Chem. A* **2006**, 110, 11781.
- (79) Dunning, T. H., Jr. *J. Chem. Phys.* **1989**, 90, 1007.
- (80) Kendall, R. A.; Dunning, T. H., Jr.; Harrison, R. J. *J. Chem. Phys.* **1992**, 96, 6796.

CT1000999